COMPARISON OF EDGE DETECTION AND HOUGH TRANSFORM TECHNIQUES FOR THE EXTRACTION OF GEOLOGIC FEATURES

D. P. Argialas and O. D. Mavrantza

Laboratory of Remote Sensing, School of Rural and Surveying Engineering, National Technical University of Athens, Greece, Heroon Polytechneiou 9, Zografos Campus, 157 80, Athens – rannia@survey.ntua.gr, argialas@central.ntua.gr

Commission III, WG4

ABSTRACT:

Photointerpretation of geologic lineaments is a subjective process. Therefore there is a need for automation of lineament mapping using optimal edge detection techniques. Efforts made in this direction include the application of Sobel and Prewitt operators or directional detectors followed by edge linking techniques (e.g. the HOUGH Transform). It is difficult to choose optimal detectors, however, since the complex scenes portrayed on satellite images are strongly dependent on the radiometric and physical properties of the sensors and on the illumination properties and topographic relief of each scene. Therefore, the geographic region determines the "suitability" of an edge detector in geologic feature extraction. In this context, the objective of this work was the implementation, evaluation and comparison of selected optimal edge detectors and the HOUGH transform algorithm towards automated geologic feature mapping in a volcanic geotectonic environment. The test area was the Nisyros Island (Greece). A LANDSAT 5 - TM image and the DEM of the study area were geometrically corregistered with the scanned topographic map of the same area. The following edge detectors were applied and assessed on band 5 of the LANDSAT-TM image and the DEM, namely, (a) Canny, (b) Rothwell, (c) Black, (d) Bezdek, (e) Iverson-Zucker, (f) *EDISON* and (g) *SUSAN*. Modified versions of the HOUGH transform were additionally applied to these data. The resulted edge maps were quantitatively assessed with the use of evaluation metrics. Finally, the performance and behaviour of each algorithm for geologic feature extraction on the specific geotectonic terrain was investigated.

1. INTRODUCTION

Geologic lineament mapping is considered as a very important issue in problem solving in Engineering, especially, in site selection for construction (dams, bridges, roads, etc), seismic and landslide risk assessment (Stefouli et.al., 1996), mineral exploration (Rowan and Lathram, 1980), hot spring detection, hydrogeological research, etc. (Sabins, 1997).

Lineament photointerpretation is a quite subjective process, requires expertise, training, scientific skills and is time consuming and expensive. Therefore, the need arises for automation of photointerpretation in order to reduce subjectivity and to help the analysts. This can be achieved using computer-assisted techniques, e.g. image processing and analysis techniques, pattern recognition and expert systems.

1.1 Edge Detection Operators: Overview

In image processing and computer vision, edge detection treats the localization of significant variations of a gray level image and the identification of the physical and geometrical properties of objects of the scene. The variations in the gray level image, commonly include discontinuities (step edges), local extrema (line edges) and junctions. Most recent edge detectors are autonomous and multi-scale and include three main processing steps: smoothing, differentiation and labeling. The edge detectors vary according to these processing steps, to their goals, and to their mathematical and computational complexity (Ziou and Tabbone, 1997).

In the present work, only step edge detectors were examined, which can generally be grouped into three major categories:
1. Early vision edge detectors (Gradient operators, e.g. the detectors of Sobel and Kirsch).
2. Optimal detectors (e.g. the Canny algorithm, etc.).
3. Operators using parametric fitting models (e.g. the detectors of Haralick, Nalwa-Binford, Nayar, Meer and Georgescu, etc) (Ziou and Tabbone, 1997).

1.2 Edge Linking Techniques: Overview

The HOUGH Transform is considered as a very powerful tool in edge linking for line extraction. Its main advantages are its insensitivity to noise and its capability to extract lines even in areas with pixel absence (pixel gaps). The Standard HOUGH Transform (SHT) proposed by Duda and Hart (Duda and Hart, 1972) is widely applied for line extraction in natural scenes, while some of its modifications have been adjusted for geologic lineament extraction purposes (Karnieli, et.al., 1996; Fitton and Cox, 1998).

In the present work, a modified Hough Transform was applied in the satellite image and the DEM, namely the Fitton-Cox algorithm. This algorithm has successfully been applied to a sedimentary terrain covered with prominent joints. Its main advantage was the extraction of small line segments, which was controlled by the input parameters (Fitton and Cox, 1998).

1.3 Lineament Extraction and Mapping: Overview

Concerning the semi-automatic and automatic lineament extraction, there are three main categories of processes:
1. The enhancement of geological line segments with the use of linear and non-linear spatial filters, such as directional gradients, Laplacian filters, and the Sobel and Prewitt operators (Morris, 1991; Mah et.al., 1995; Philip, 1996; Süzen, and Toprak, 1998), as well as morphological filters (Tripathi et.al., 2000).

2. The semi-automatic and automatic lineament extraction methods, such as edge following, graph searching (Wang and Howarth, 1990) and edge linking operators (standard and modified Hough Transform) (Cross, 1988; Karnieli et.al., 1996; Fitton and Cox, 1998), novel edge tracing algorithms (STA, START and ALERT algorithm) (Koike et.al., 1998).

3. The design of a knowledge-based system, which could take the measurable lineament information (length, aspect) from a DEM into account (Morris, 1991).

1.4 Motivation and aim

From the thorough examination of the literature it is inferred that computer-assisted methods for the detection of structural (tectonic) lineaments (namely faults and joints), were exclusively based on edge enhancement or spatial filtering techniques (directional and / or gradient filters). These methods produced edge maps requiring further processing (thresholding and thinning) for the linear segments to appear with one-pixel thickness. Optimal edge detectors (e.g. the Canny algorithm) have already been successfully applied on natural scenes with quite satisfactory results (binary images with one-pixel thickness, efficient length and pixel connectivity), and this makes their application in geologic lineament mapping more tempting and worth investigating. Furthermore, length is stated as a crucial statistical parameter for lineament interpretation and classification and optimal edge detection techniques can produce segments with sufficient length.

The implementation of the selected edge detectors on a satellite image of a hydrothermal volcanic field has already been investigated by the authors (Mavrantza and Argialas, 2003), and the results were quite promising. Since only early vision operators such as SOBEL, Laplace and Prewitt have been applied to date for lineament extraction, further application on a DEM is promising. A furthermore comparison of edge detection outputs to those of HOUGH Transform with evaluation metrics was also required in order to investigate the applicability of these methods for lineament extraction.

2. METHODOLOGY

2.1 Study area and data used

For the implementation and quantitative evaluation of the applied edge detection algorithms and the HOUGH transform for lineament mapping, a geothermal terrain was selected, e.g., the Island of Nisyros, which is located in the volcanic back-arc of the Dodekanesse Complex, Aegean Sea, Greece. Nisyros is a Quaternary strato-volcano, which is characterized by a well developed caldera. The major part of this caldera is filled with dacitic and rhyodacitic domes, while andesitic and pillow-lavas are also present. The tectonic regime of this area is defined by two major trends in the NW and in the NE direction (PENED99, 2000).

The data used in the present work were: (a) Band 5 of a LANDSAT 5-TM image acquired on August 10, 1991, (b) a scanned topographic map with a scale of 1:50.000, and (c) the Digital Elevation Model of the same area with 5m spacing.

2.2 Image pre-processing

In the pre-processing stage, a LANDSAT 5-TM satellite image and the DEM of the same area were geometrically corregistered with the scanned topographic map of the same area (with a scale of 1:50.000) and geodetically transformed into the Transverse Mercator Projection and the Hellenic Geodetic Datum (HGRS87). Band 5 of the LANDSAT 5-TM image was selected for the implementation of the edge detection algorithms, because of its usefulness in lithological and structural mapping (Woldai, 1995). This band was initially contrast-stretched using a linear transform so as to achieve a visually better image for input into the edge detection algorithms.

For the implementation of the Pratt evaluation metric, an ancillary ground truth (reference) file was required as input. This ground truth file contained all the visually interpreted lineaments from the satellite image (and verified on the ground), represented with their X, Y coordinates and the total number of the actual edge points (in an ASCII format file).

2.3 Optimal edge detection algorithms: Implementation

For each algorithm, the combinations of input parameter sets were selected based on trial-and-error experiments and assessed (a) using mostly the evaluation measures of Pratt and Rosenfeld (Abdou and Pratt, 1979; Kitchen and Rosenfeld, 1981) (which will be explained in section 2.5.), and (b) by evaluating the optical correspondence to the ground map (Figure 1). Due to the restricted paper length, only the best results of each category are presented.
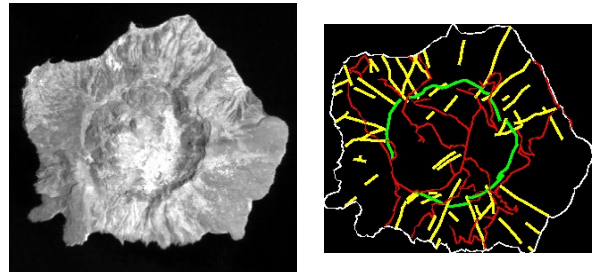

Figure 1: Left: Initial band TM-5 of the Nisyros caldera. Right: Ground map illustrating faults (yellow), morphostructural segments delineating the caldera crater (light green), coastline (white), and road network (red) (For color, see CD).

For the *Canny* algorithm, the parameter set with the highest score of the Pratt evaluation metric (0.4680) (Table 1) was for σ=1.25, T*low*=0.40 and T*high*=0.70.

For the *Rothwell* algorithm, the following combination of input parameters was the optimal: σ=2.00, *Tlow*=6.00 and *a*=0.90 (Figure 2). This parameter set produced a Pratt metric of 0.4508 (Table 1):
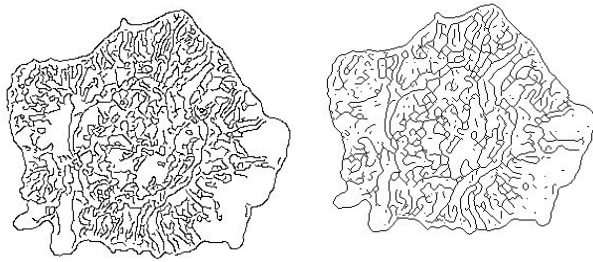
Figure 2: Left: The Canny output map. Right: The Rothwell edge map.

The input parameters to the *Iverson-Zucker* algorithm were the following: a) Threshold (*T*), number of directions (*d*) for the algorithm to follow (1-16), degrees of freedom based upon the number of directions (4-64), the output detection type (E (edges), P (Positive lines), and N (Negative lines)). The best output result (0.4967) (Table 1) was derived using 16 directions and *T*=0.015.

The input parameter to the *Black* algorithm was the smoothing coefficient (σ) in the range (0, 1]. The best output edge map resulted in the highest Pratt metric (0.4773) (Table 1) using σ=0.25 (Figure 3).
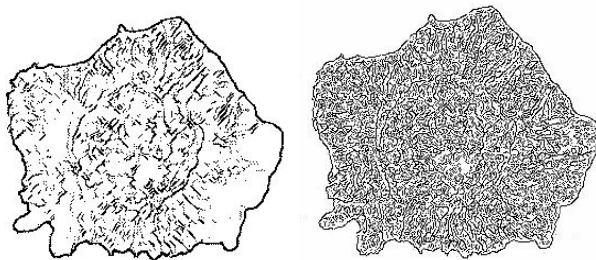

Figure 3: Left: The Iverson-Zucker output map. Right: The Black edge map.

The input parameters to the *SUSAN* algorithm by Smith and Brady were: (a) Brightness threshold (-*T*) (default = 20), (b) distance threshold (-*d*) (default = 4.00) (used instead of flat 3x3 mask), (c) use of flat 3x3 mask (-3), (d) choice among edges (-e), smoothing (-s) or corner detection (-c) modes. The best output result (0.3171) (Table 1) was derived for *T*=15.00 (Figure 4).
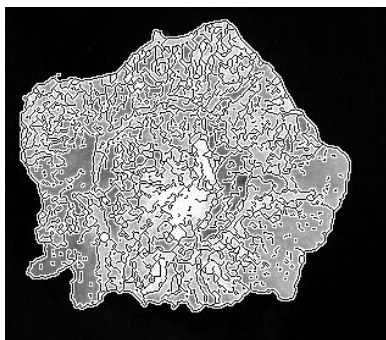

Figure 4: The SUSAN output map. The edges are depicted with black lines and overlayed on the smoothed image.

Using the *EDISON* algorithm, the best output edge map (0.4507) (Table 1) was derived using the following combination of parameters: a) Gradient=2.00, b) Minimum length=5.00, c) – e) Nonmaxima suppression: *Type*=arc, Rank=0.5 and Confidence=0.4, f) – h) High Threshold for hysteresis: *Type* = box, Rank=0.91 and Confidence=0.92, and finally, i) – k) Low Threshold for hysteresis: *Type*=arc, Rank=0.98 and Confidence=0.93.

Finally, the parameters used in the Bezdek algorithm are: *(1) Tau*, in the range [0.0…5.0], *(2) Chi*, as a function *f(Tau)=2.0*Tau*, *(3) Gamma*, as *f(Tau)=2.0*Tau*, *(4) Omega,* as function of *f(Tau)=3.0*Tau*, *(5) Binary Threshold*, which is in the range [0…GRAY LEVELS − 1] and *(6) Edge Features* (Sobel). The best result (0.4428) (Table 1) was obtained for *Tau*=1.00 and *Binary Threshold*=80.00 (Figure 5).
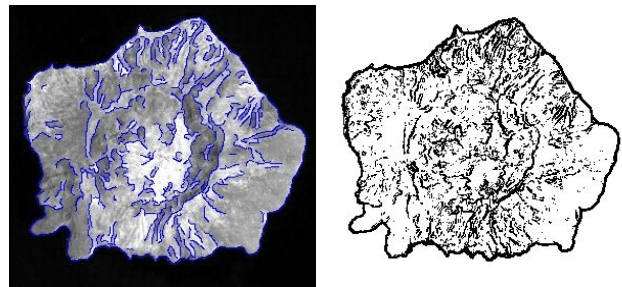

Figure 5: Left: The EDISON edge map. Right: The Bezdek edge map.

In a similar manner and logic, the selected edge detection algorithms were further applied on the DEM of the same area, and, only two of the best results as judged by photointerpretation (Table 1) are presented in Figure 6 due to paper size constraints.
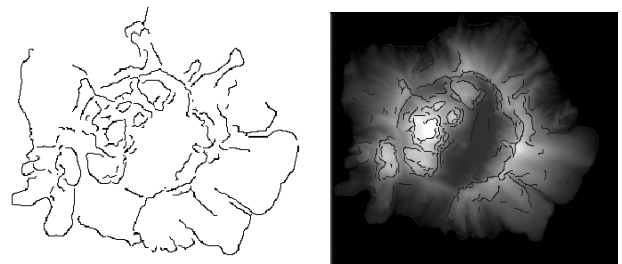

Figure 6: (a) Based on DEM processing: the Canny edge map (left) and the EDISON edge map (right).

In the Canny algorithm, the parameter set with the highest score of the Pratt evaluation metric (0.4332) (Table 1) was for σ=1.50, T*low*=0.30 and T*high*=0.70.

In the EDISON algorithm, the best output edge map (0.4359) (Table 1) was derived using the following combination of parameters: a) Gradient=2.00, b) Minimum length=4.00, c) – e) Nonmaxima suppression: *Type*=arc, Rank=0.5 and Confidence=0.7, f) – h) High Threshold for hysteresis: *Type* = box, Rank=0.93 and Confidence=0.96, and finally, i) – k) Low Threshold for hysteresis: *Type*=arc, Rank=0.97 and Confidence=0.93 (Figure 6).

2.4 The HOUGH Transform: Implementation

According to Fitton and Cox (Fitton and Cox, 1998), before the application of the Hough Transform, several binary edge maps could be tested, that have been derived using diverse pre-processing methods. In this work, three different pre-processing methods were tested. The first method (Method A') is the method initially proposed by the authors (edge enhancement / gain-control filtering / thresholding / Zhang-Suen thinning). Method B' was based on applying an enhanced Sobel filter, followed by thresholding and thinning. Finally, Method C' was based on a 3x3 grayscale morphological dilation, followed by applying an isotropic filter and thresholding. The input parameters to the Fitton-Cox algorithm that produced the highest Pratt value on the satellite image (Table 1) were: (a) Method C', (b) *cutoff h* (%) =30, and, (c) *normalization factor k*=1.0. For the DEM, the input parameters to the Fitton-Cox algorithm that produced the highest Pratt value (Table 1) were: (a) Method A', (b) *cutoff h* (%) =85, and, (c) *normalization factor k*=3.5.
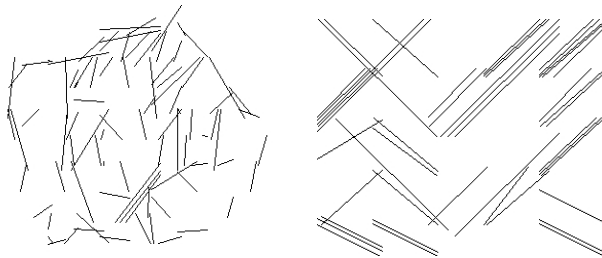

Figure 7: The lineament map extracted by Fitton-Cox algorithm on the satellite image (left) and the DEM (right).

2.5 Performance evaluation measures of the edge detection algorithms: Description and implementation

For the quantitative evaluation and assessment of the employed edge detection algorithms, two evaluation metrics were used:

- The *Rosenfeld evaluation metric (E1)*: This evaluation scheme is based on the local edge coherence and measures how well an edge fits to the local neighborhood of edge pixels but it does not concern itself with the actual position of the edge, therefore it is a supplement to Pratt's evaluation metric (Kitchen and Rosenfeld, 1981; Parker, 1997).
- *The Pratt evaluation metric (E2):* This metric is a formulated function of the distance between correct and measured edge positions, but it is also indirectly related to the false positive and false negative edges. Pratt's metric is considered to be a performance evaluation measure that requires ground truth files. Therefore, it is directly related to the actual position of the edge pixels and serves as a more objective quantitative evaluation measure (Abdou and Pratt, 1979; Parker, 1997).

In the following table the performance evaluation of edge detection algorithms and the HOUGH Transform (Fitton-Cox algorithm) is presented for the satellite image and the corresponding DEM (Table 1):

ALGORITHMS	*PRATT / ROSENFELD* METRICS ON LANDSAT TM-5	*PRATT / ROSENFELD* METRICS ON THE DEM
CANNY	0.4680 / 0.6263	0.4332 / 0.6494
ROTHWELL	0.4508 / 0.6529	0.4693 / 0.6318
BLACK	0.4773 / 0.5765	0.4642 / 0.6364
SUSAN	0.3171 / 0.6097	0.3068 / 0.8003
IVERSON-ZUCKER	0.4967 / 0.6297	0.2635 / 0.7357
BEZDEK	0.4428 / 0.6595	0.4286 / 0.7442
EDISON	0.4507 / 0.6379	0.4359 / 0.6513
FITTON-COX	0.3017 / 0.7858	0.3716 / 0.7824

Table 1: Performance evaluation metrics (Rosenfeld and Pratt) for the satellite image and the DEM of Nisyros Island

The Canny and Rothwell algorithms can be found at ftp://figment.csee.usf.edu/pub/Edge_Comparison/source_code. The *EDISON* algorithm can be found at the address: http://www.caip.rutgers.edu/riul/. The *SUSAN* algorithm can be found at http://www.fmrib.ox.ac.uk/~steve/susan/. The Iverson-Zucker algorithm can be found at ftp://ftp.cim.mcgill.ca/pub/people/leei/loglin.tar.gz. The algorithm by Black and that of Bezdek can be found at http://marathon.csee.usf.edu/edge/edgecompare_main.html.
The modified HOUGH transform suggested by Fitton and Cox can be obtained from the FTP site of the "*Computers and Geosciences*" Journal, Elsevier Publishing at ftp://ftp.iamg.org. More explanatory details concerning the theoretical background of the applied algorithms can be found in the corresponding papers (Canny, 1986; Rothwell, et.al., 1994; Iverson and Zucker, 1995; Black, et.al., 1998; Smith and Brady, 1997; Sutton and Bezdek, 1998; Meer and Georgescu, 2001; Fitton and Cox, 1998).

2.6 Results and Discussion

A set of optimal edge detectors for a varying combination of input parameters was applied and provided interesting results as far as their quantitative assessment is concerned.

Satellite image: For the volcanic field of Nisyros Island, all the applied algorithms provided a relative high Rosenfeld metric (local edge coherence) in a small range of values ((0.57-0.66)), and a Pratt metric in the range of (0.31-0.47). The Rosenfeld metric stands for the pixel coherence, which appears to be almost over 60% for all the applied edge detectors.

The Canny edge detector performs best with the Rothwell algorithm to follow. It also should be noted that the ground truth file used in Pratt's evaluation metric contained only the geologic lineaments, therefore the output values were not high. If this file had included all lineaments (geologic and non-

geologic), the output metric values would have been much higher (over 0.8).

Generally, from the qualitative and quantitative comparison of the HOUGH Transform by Fitton-Cox and the edge detection algorithms it is inferred that edge detection algorithms perform better in terms of Pratt quantitative evaluation, while the HOUGH Transform is superior concerning the Rosenfeld metric. The latter makes sense because the modified HOUGH Transform algorithm extracts fully connected lines using pixels.

Furthermore, the performance of the Fitton-Cox algorithm is characterized by a localization problem, meaning that the extracted lines are not accurately localized comparatively to the edge detection algorithms and, the length of the extracted lines is fully dependent on the selection of the input parameters. On the other hand, a line is what the photointerpreters represent a lineament with, and not a curvilinear segment.

3. CONCLUSIONS

One main aspect from applying the edge detection algorithms is the capability of extracting segments that really follow the terrain topography. This leads to the extraction of the exact shape of the geomorphologic features, as the caldera in this case. Taking also into consideration that these algorithms perform well in terms of coherence, edge localization and high edge response, the implementation of edge detection algorithms provides useful means towards automated lineament mapping.

Finally, the HOUGH Transform is quite useful for line extraction, but it requires a proper parameter setting and adjustments to be applicable in different terrain and illumination conditions of natural scenes when applied to satellite data. Its performance to the Digital Elevation Model could be further investigated.

4. REFERENCES

Abdou, I. E. and W. K. Pratt, 1979. Quantitative Design and Evaluation of Enhancement / Thresholding Edge Detectors. *Proceedings of IEEE*, 67(5), pp. 753-763.

Bezdek, J. C., R. Chandrasekhan and Y. Attikiouzel, 1998. A geometric approach to edge detection. *IEEE Transactions. on Fuzzy Systems,* 6, pp. 52-75.

Black, M., G. Sapiro, D. Marimont and D. Heeger, 1998. Robust Anisotropic Diffusion. *IEEE Transactions on Image Processing*, 7, pp. 421-432.

Canny, J. F., 1986. A computational approach to edge detection. *IEEE Transactions. on Pattern Analysis and Machine Intelligence*, 8, pp. 679-714.

Cross, A. M., 1988. Detection of circular geological features using the Hough Transform. *International Journal of Remote Sensing*, 9, pp. 1519-1528.

Duda, R. O. and P. E. Hart, 1972. Use of the Hough Transform to detect curves and lines in pictures. *Communications of the Association for Computing Machinery*, 15(1), pp. 11-15.

Fitton, N. C. and S. J. D. Cox, 1998. Optimizing the application of the Hough Transform for the automatic feature extraction from geoscientific images. *Computers and Geosciences,* 24, pp. 933-951.

Iverson, L. A. and S. W. Zucker, 1995. Logical / linear operators for image curves. *IEEE Transactions on Pattern Analysis and Machine Intelligence*, 17(10), pp. 982-996.

Jensen, J. R. 1996. *Introductory Digital Image Processing,* Prentice–Hall Series, New York, pp. 162-165.

Karnieli, A., A. Meisels, L. Fisher and Y. Arkin, 1996. Automatic extraction and evaluation of geological linear features from digital remote sensing data using a Hough Transform. *Photogrammetric Engineering and Remote Sensing*, 62, pp. 525-531.

Kitchen, L. and A. Rosenfeld, 1981. Edge Evaluation using Local Edge Coherence. *IEEE Transactions on Systems, Man and Cybernetics*, 11(9), pp. 597-605.

Koike, K., S. Nagano and K. Kawaba, 1998. Construction and Analysis of Interpreted Fracture Planes through Combination of Satellite-Image Derived Lineaments and Digital Elevation Model Data. *Computers and Geosciences*, 24, pp. 573-583.

Mah, A., G. R. Taylor, P. Lennox and L. Balia, 1995. Lineament Analysis of Landsat TM images, Northern Territory, Australia. *Photogrammetric Engineering and Remote Sensing*, 61, pp. 761-773.

Mavrantza, O. D. and D. P. Argialas, 2003. Implementation and evaluation of spatial filtering and edge detection techniques for lineament mapping - Case study: Alevrada, Central Greece. *Proceedings of SPIE International Conference on Remote Sensing: Remote Sensing for Environmental Monitoring, GIS Applications, and Geology II,* M. Ehlers (editor), *SPIE*-4886, pp. 417-428, SPIE Press, Bellingham, WA.

Meer, P. and B. Georgescu, 2001. Edge detection with embedded confidence. *IEEE Transactions on Pattern Analysis and Machine Intelligence.*, PAMI-23, pp. 1351-1365.

Morris, K., 1991. Using knowledge-base rules to map the three-dimensional nature of geological features. *Photogrammetric Engineering and Remote Sensing*, 57, pp. 1209-1216.

Rokos, D., D. Argialas, R. Mavrantza, K. ST- Seymour, C. Vamvoukakis, M. Kouli, S. Lamera, H. Paraskevas, I. Karfakis, and G. Denes, 2001. Structural analysis for gold mineralization using Remote Sensing and Geochemical techniques in a G.I.S. environment: Island of Lesvos, Hellas. *Natural Resources Research*, 9(4), pp. 277-293.

Rothwell, Ch., J. Mundy, B. Hoffman and V. Nguyen, 1994. Driving Vision by Topology. TR-2444 – Programme 4, INRIA, pp. 1-29.

Parker, J. R., 1997. *Algorithms for Image Processing and Computer Vision,* John Wiley & Sons Inc., New York, pp. 184-185.

PENED99, 2000. Exploitation of capabilities of Remote Sensing for the localization of precious metals in the geothermal fields of Lesvos and Nisyros Island using Milos Island as pilot area. Final Technical Report 99EΔ-127, General Secretariat of Research and Technology, Ministry of Development, Athens, Greece.

Perona, P. and J. Malik, 1990. Scale-space and edge detection using anisotropic diffusion. *IEEE Transactions on Pattern Analysis and Machine Intelligence**, 12, pp. 629-639.

Philip, G., 1996. Landsat Thematic Mapper data analysis for the Quaternary tectonics in parts of the Doon Valley, NW Himalaya, India. *International Journal of Remote Sensing*, 17, pp. 143-153.

Rowan, L. C. and E. H. Lathram, 1980. Mineral Exploration. Chapter 17, in *Remote Sensing in Geology* (B. S. Siegal and A. R. Gillespie, editors), John Wiley and sons, New York, pp. 553-605.

Sabins, F. F., 1997. *Remote Sensing: Principles and Interpretation*. W. H. Freeman and Company, New York, p. 361.

Smith, S. M. and J. M. Brady, 1997. SUSAN-A New Approach to Low Level Image Processing. *International Journal of Computer Vision*, 23(1), pp. 45-78.

Stefouli, M., A. Angellopoulos, S. Perantonis, N. Vassilas, N. Ambazis, E. Charou, 1996. Integrated Analysis and Use of Remotely Sensed Data for the Seismic Risk assessment of the southwest Peloponessus Greece. *First Congress of the Balkan Geophysical Society,* 23-27 September, Athens Greece.

Sutton, M. A. and J. Bezdek, 1998. Enhancement and analysis of digital mammograms using fuzzy models. In *Proceedings of the 26th Applied Imagery and Pattern Recognition (AIPR) Workshop: Exploiting New Image Sources and Sensor,* J. M. Selander, SPIE-3240, pp.179-190, SPIE Press, Bellingham, WA.

Süzen, M. L. and V. Toprak, 1998. Filtering of satellite images in geological lineament analyses: an application to a fault zone in Central Turkey. *International Journal of Remote Sensing*, 19, pp. 1101-1114.

Tripathi, N. K., K. V. G. K. Gokhale and M. U. Siddiqu, 2000. Directional morphological image transforms for lineament extraction from remotely sensed images. *International Journal of Remote Sensing*, 21, pp. 3281-3292.

Wang, J. and P. J. Howarth, 1990. Use of the Hough transform in automated lineament detection. *IEEE Transactions. on Geoscience and Remote Sensin*g, 28, pp. 561-566.

Woldai, T., 1995. Multiple-source remotely sensed data for lithologic and structural mapping. *ITC Journal*, 2, pp, 95-113.

Ziou, D. and S. Tabbone, 1997. Edge Detection Techniques – An Overview. *TR-195,* Département de Math et Informatique, Université de Sherbrooke, Québec, Canada, pp. 1-41.